

results) that this mechanism (eq 2) does not account for exchange at pH <4 in adenosine compounds, since the resulting values of  $k_B$  in eq 2 are at variance by two orders of magnitude with those expected from buffer data. These workers showed that consistent kinetic parameters are obtained only for cytidine compounds, whose exchange at pH <4 is quite slow, producing virtually no pH broadening at pH <2. In addition, low pH broadening is seen for both m<sup>7</sup>G (Figure 4) and m<sup>1</sup>A (McConnell and Politowski, unpublished results), which suggests direct exocyclic amino protonation as opposed to endocyclic protonation as a chief mechanism for purine amino exchange at low pH. The formation of an amino-protonated intermediate is consistent with the decrease in low pH exchange upon endocyclic methylation (Figure 4) since this substitution would decrease the basicity of -NH<sub>2</sub>.

Some new implications of these results on guanine can be mentioned with respect to the mechanism of exchange in polynucleotides. First, the exchange mechanism postulated for amino protons in polynucleotides (Teitlebaum & Englander, 1975) is not general for all nucleobases. Endocyclic protonation does not provide a general buffer-catalyzed exchange route for the guanine amino protons, whose rates would be catalyzed chiefly by hydroxyl ion involving the neutral, unprotonated base. Therefore, the large effect of imidazole on all exchange classes of DNA may require interactions of a special type, e.g., intercalation (McConnell & von Hippel, 1970). Second, the large difference in effect of buffers on amino exchange in adenine, cytosine, and guanine should provide a means for the assignment of amino <sup>1</sup>H NMR resonance in aqueous self-complementary oligonucleotides [see, for example, Patel (1977)]. Third, an inverse relationship, conceived between amino H-bond strength and helical stability, was based on a notion that base pairing in helix formation might require weak hydrogen bonding with competing water molecules (McConnell, 1978b). On this basis the expected increase in amino acidity following guanine N-7 protonation

was postulated as a mechanism for in vivo destabilization of G-C-rich regions in DNA. This speculated mechanism does not appear to be supported by these results, which show that the increase in guanine amino acidity with N-7 protonation is much smaller than expected. Weak amino to water hydrogen bonding might not be altered greatly in guanine through N-7 interactions, which is borne out by the comparison of the <sup>1</sup>H NMR spectra of 2',3'-cGMP and m<sup>7</sup>G (Figure 5).

**Registry No.** 2',3'-cGMP, 634-02-6; 7-methylguanosine, 20244-86-4; phosphate, 14265-44-2; acetate, 64-19-7.

## References

- Crooks, J. E. (1975) in *Proton Transfer Reactions* (Caldin, E. F., & Gold, V., Eds.) pp 153-177, Wiley, New York.
- Cross, D. G., Brown, A., & Fisher, H. F. (1975) *Biochemistry* 14, 2747.
- Eigen, M. (1964) *Angew. Chem., Int. Ed. Engl.* 1, 1.
- Hoo, D.-L., & McConnell, B. (1979) *J. Am. Chem. Soc.* 101, 7470.
- Jones, J. W., & Robins, R. K. (1963) *J. Am. Chem. Soc.* 85, 193.
- McConnell, B. (1974) *Biochemistry* 13, 4516.
- McConnell, B. (1978a) *Biochemistry* 17, 3168.
- McConnell, B. (1978b) in *Nuclear Magnetic Resonance in Molecular Biology* (Pullman, B., Ed.) p 147, Reidel Publishing Co., Dordrecht, Holland.
- McConnell, B., & von Hippel, P. H. (1970) *J. Mol. Biol.* 50, 297.
- McConnell, B., & Seawell, P. C. (1972) *Biochemistry* 11, 4382.
- Patel, D. J. (1977) *Biopolymers* 16, 1635.
- Pinnavaid, T. J., Miles, H. T., & Becker, E. D. (1975) *J. Am. Chem. Soc.* 97, 7178.
- Redfield, A. G. (1978) *Methods Enzymol.* 49, 253.
- Teitlebaum, H., & Englander, S. W. (1975) *J. Mol. Biol.* 92, 55.

## Sequence-Specific Recognition of Deoxyribonucleic Acid. Chemical Synthesis and Nuclear Magnetic Resonance Assignment of the Imino Protons of λ O<sub>R</sub>3 Operator Deoxyribonucleic Acid<sup>†</sup>

Shan-Ho Chou, Dennis R. Hare, David E. Wemmer, and Brian R. Reid\*

**ABSTRACT:** Using solid-phase phosphite triester methods, we have synthesized both strands of the phage λ O<sub>R</sub>3 DNA sequence, reannealed them, and studied the native operator duplex by high-resolution NMR at 500 MHz. At 7 °C the imino protons of the two terminal base pairs at each end have disappeared from the spectrum by exchange broadening. The 13 detectable imino resonances have been assigned to their respective base pairs in the duplex by using sequential near-

est-neighbor NOE connectivity methods described previously. In cases where two imino protons overlap in the spectrum, spin diffusion was used to drive the cross-saturation further afield in order to produce second-order next-nearest-neighbor effects. The results show that the imino connectivity method can be used to unambiguously assign the imino proton spectrum of operator DNAs containing one to two full turns of the helix.

**T**he recognition of short stretches of specific DNA sequences such as operators and promoters is of central importance in

the control of gene expression. Operators consist of approximately 20 base pairs at the proximal end of genes or operons and are specifically recognized and bound by repressor proteins; several bacterial and viral operators have been characterized with respect to sequence and the binding affinity of their corresponding repressors (Bourgeois & Pfahl, 1976).

The right operator locus O<sub>R</sub> of bacteriophage λ is a par-

<sup>†</sup> From the Chemistry Department and Biochemistry Department, University of Washington, Seattle, Washington 98195. Received March 22, 1983. This work was supported by instrumentation grants from the Murdock Foundation, the National Science Foundation (PCM80-18053), and the National Institutes of Health (GM2874-O1S1).

ticularly interesting example which has been studied in detail by Ptashne, Sauer, and their co-workers (1980). It contains three discrete 17 base pair operators designated  $O_{R1}$ ,  $O_{R2}$ , and  $O_{R3}$  to which  $\lambda$  repressor and cro protein bind. Cro protein binds preferentially to  $O_{R3}$  whereas repressor binds preferentially to  $O_{R1}$  and  $O_{R2}$ . The  $\lambda$  repressor protein is required to maintain lysogeny of the virus whereas cro protein is essential for lytic phage growth. The complete DNA sequence of the  $O_R$  region has been determined and several operator-constitutive point mutations which markedly reduce the protein binding affinity have been characterized. Recently a molecular model of the cro- $O_{R3}$  interaction has been inferred from the crystal structure of cro protein (Ohlendorf et al., 1982).

NMR spectroscopy is a particularly informative technique for studying structure and dynamics of RNA and DNA (Reid, 1981; D. J. Patel et al., 1982; Hare & Reid, 1982a,b; Feigon et al., 1982). The hydrogen bonds between complementary base pairs can be studied in  $H_2O$  by using solvent suppression methods, and many of these have been assigned by using nearest-neighbor connectivity methods in tRNA (Hare & Reid, 1982a,b; Roy et al., 1982) and, to a lesser extent, in DNA (D. J. Patel et al., 1982). Very recently two-dimensional NMR<sup>1</sup> methods have been applied to short DNA sequences in  $D_2O$  solutions (Feigon et al., 1982) and, with more refinement, should lead to the assignment of many of the non-exchangeable CH protons. To date only one NMR study of DNA sequences related to biological operators has been reported in which Zuiderweg et al. (1981) assigned the imino protons of base pairs in two DNA fragments containing the left half and the right half of the *lac* operator sequence. A major stumbling block in such studies is the availability, in NMR quantities, of operator DNA sequences of 15–25 base pairs in length. This bottleneck has now been eliminated by the recent development of solid-phase phosphite triester methods (Matteucci & Caruthers, 1981; Beaucage & Caruthers, 1981; Chow et al., 1981; Tanaka & Letsinger, 1982) for the preparative synthesis of defined DNA sequences.

In the present paper we report the complete synthesis of the  $\lambda$   $O_{R3}$  operator (+) and (–) strands using solid-phase phosphite triester methods. The hydrogen-bonded imino protons of this operator duplex have been assigned to their specific base pairs by the same imino NOE connectivity “sequencing” methods used to assign imino protons in tRNA helices (Hare & Reid, 1982a,b).

## Materials and Methods

**DNA Synthesis.** Deoxyadenosine, deoxyguanosine, deoxycytosine, and thymidine were purchased from Biosearch (San Rafael, CA). N-Blocked 5'-DMT deoxynucleosides were prepared according to Ti et al. (1982) and Narang et al. (1980). These were derivatized to silica gel according to Chow et al. (1981). 3'-Phosphoramidites were prepared by the procedure of Beaucage & Caruthers (1981). The resulting N-blocked 5'-DMT 3'-phosphoramidites were found to be at least 95% pure by <sup>31</sup>P NMR. Just prior to use the phosphoramidites were activated by the addition of tetrazole amidite activator (Biosearch, San Rafael, CA).

**NMR Spectroscopy.** Duplex  $O_{R3}$  operator DNA (14 mg) was dissolved in 0.4 mL of 10 mM sodium phosphate buffer, pH 7.0, and transferred to a 5-mm NMR tube. Spectra were obtained on a modified Bruker WM500 spectrometer with

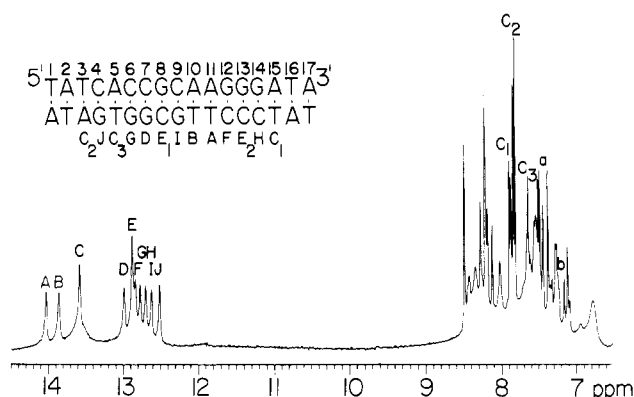


FIGURE 1: Low-field region of the 500-MHz NMR spectrum of the  $\lambda$   $O_{R3}$  duplex at 7 °C in 10 mM sodium phosphate, pH 7. Peaks A–J in the 11–15 ppm region are imino protons hydrogen bonded between complementary base pairs; the 7–9 ppm region contains amino protons and carbon-bonded aromatic protons of the bases. The sequence of base pairs in  $O_{R3}$ , numbered from 1 to 17, is shown above the spectrum together with the assignment of each base pair to its particular imino resonance (see text).

DSS as internal reference by using a modified Redfield 21412 observation pulse to suppress the large  $H_2O$  resonance. Usually 600 pulses were signal averaged at a rate of 2.5 pulses/s and Fourier transformed to obtain the frequency spectrum. NOE difference spectra were obtained by interleaving selectively saturated and off-resonance-irradiated FID's as described previously (Hare & Reid, 1982a,b). Imino protons were saturated for 0.4–0.8 s to allow buildup of cross-saturation. All chemical shifts are referenced to internal DSS.

## Results

The heptadecameric oligodeoxynucleotide dTATCACCGCAAGGGATA and its complementary strand dTATCCCTTGGCGTGATA were prepared separately from silica-dA by using a capped sintered glass filter funnel as the reaction vessel (M. H. Caruthers and M. Insley, personal communication). The complete cycle for addition of one residue consisted of 1 min of detritylation with 2%  $Cl_3CCO-OH$ , 5 min of coupling, 2 min of oxidation with iodine/water, 2 min of capping with acetic anhydride, and four washes with acetonitrile between steps. After 16 cycles the heptadecamer was treated with thiophenol/triethylamine at room temperature for 90 min to remove methyl groups from the phosphotriesters. The oligomer was then removed from the silica and deprotected by incubating in 29.4% ammonia at 60 °C overnight. The product was concentrated and applied to TLC plates (silica gel 60 F<sub>254</sub>). After the plates were developed in ammonia/1-propanol/water (35/55/10) for 12 h, the slowest moving band was cut out and eluted with 5 mL of 0.5 N ammonium bicarbonate three times. Low, but detectable, levels of all 16 smaller oligomers were observed under a UV lamp as bands preceding the major dark heptadecamer. Equal amounts of the two purified heptadecadeoxynucleotides were combined and heated in a water bath at 80 °C for 3 min. After being cooled to room temperature over a period of 20 min, the reannealed duplex was lyophilized to a dry white powder. The yield of final pure duplex from 10  $\mu$ mol of silica-dA was 14 mg (280  $A_{260}$  units).

**NMR Assignments.** The spectrum of the  $\lambda$   $O_{R3}$  operator duplex at 7 °C in 10 mM phosphate buffer is shown in Figure 1. In the imino proton spectral region there are 10 resolved peaks between 14 and 12.4 ppm with a total intensity of 12–13 protons. Peak E contains two protons and peak C contains

<sup>1</sup> Abbreviations: DMT, dimethoxytrityl; NOE, nuclear Overhauser effect; NMR, nuclear magnetic resonance;  $Cl_3CCOOH$ , trichloroacetic acid; TLC, thin-layer chromatography; DSS, 4,4-dimethyl-4-silapentane-1-sulfonate.

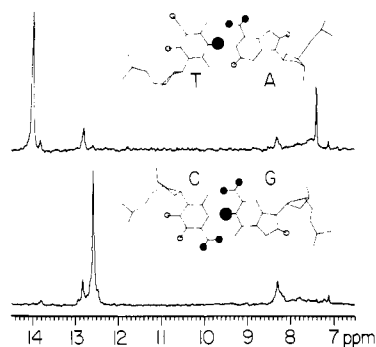


FIGURE 2: Watson-Crick base pairs and their imino NOE patterns. Imino protons are shown as large filled circles, amino protons as small filled circles, and carbon protons as open circles. (Upper) the imino proton of an AT pair is adjacent to a carbon-bonded proton (adenine C2H) and hence gives an NOE to a narrow CH resonance in the 7–9 ppm region when saturated. (Lower) the GC imino proton has only amino protons surrounding it and therefore gives NOEs in the 7–9 ppm region that are broadened due to relaxation by  $^{15}\text{N}$ .

two to three protons. When the temperature is lowered to 0 °C, additional intensity corresponding to three to four extra protons appears in the 13.4–13.6 ppm region. We thus conclude that at 7 °C in this low ionic strength four AT base pairs (probably 1, 2, 16, and 17) have helix lifetimes that are shortened to the extent that they no longer generate discrete low-field resonances.

In order to determine base pair type and nearest neighbors, each imino resonance was selectively saturated in turn. Base pair type can be established from the presence or absence of narrow-line CH NOEs in the 7–9 ppm region. As shown in Figure 2, only AT imino protons have an adjacent CH to cross-saturate (the adenine C2H); GC imino protons are surrounded by amino protons which give broad-line NOEs in the 7–9 ppm region (Hare & Reid, 1982a,b). An example of such analyses, and the logic which leads to the assignments, is presented in Figure 3. The middle two difference spectra show the effects of separately saturating the two lowest field imino peaks A and B. From the narrow C2H NOEs in the 7–8 ppm region, both A and B are obviously AT pairs as was expected from their chemical shifts of 14 and 13.8 ppm. The small imino-imino NOEs from A to B and from B to A establish that these two AT pairs are nearest neighbors. Although A and B have similar chemical shifts, they are separated by 90 Hz at 500 MHz which is ample separation to permit saturation of B alone without spillover irradiation of A; this was confirmed by the absence of A saturation when the decoupler was set 90 Hz on the other side of peak A.

The distal neighbor of B is obviously I (a GC pair—only amino NOEs in the 8 ppm region), and it is equally obvious that peak E (two protons—both GC pairs) is the other neighbor of I. Besides B, peak F is a neighbor of A, and saturation of F reveals that it is a GC pair. Thus the two nearest-neighbor AT pairs A and B each have a GC pair outside them. This configuration occurs only once in the  $\text{O}_R3$  sequence, thus establishing that AT10 and AT11 must be peaks A and B without knowing from first principles which is which. However, as a structural consequence of the right-handedness of native DNA, irradiation of the AT10 imino proton should cross-saturate the adenine C2H of both AT10 and AT11, whereas saturation of the AT11 imino proton should cross-saturate *only* the C2H of AT11 but not the AT10 C2H which is too far removed (see Figure 4). Experimentally it is peak B that cross-saturates two separate C2H's (7.4 and 7.15 ppm) whereas peak A only gives a CH NOE to the 7.4 ppm C2H; hence the data strongly suggest that peak B is

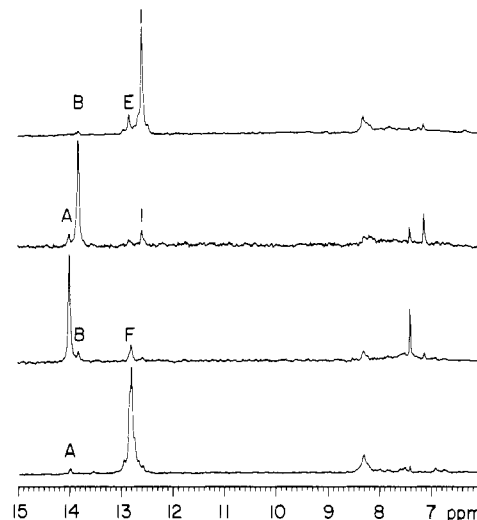


FIGURE 3: (Top to bottom) NOE connectivity from peaks I to B to A to F. From the intrabase pair effects in the 7–9 ppm region, peaks I and F are GC pairs whereas A and B are AT pairs. Note that peak B cross-saturates two adenine C2H resonances, the higher field member of which is not excited by saturation of peak A.

AT10 and peak A is AT11, but this interpretation rests on the assumption that the helix is right-handed.

Foregoing any assumptions, at this stage of the assignment we have established that the GC pairs I and F surround AT10 and AT11 in a connectivity train I-B-A-F which corresponds either to base pairs 9-10-11-12 or base pairs 12-11-10-9. Careful irradiation on the upfield side of F suggested a probable NOE to E, and saturation of peak I also revealed an NOE to E (peak E contains two protons, both of which are GC pairs). We thus have the unfortunate circumstance in which one of the protons in E is a next nearest neighbor of peak A and the other proton in E is a next nearest neighbor of peak B. Thus peak E contains both GC8 and GC13. Saturation of peak E (two protons) gave four NOEs, the two expected ones to F and I and two new ones to H and D. At this stage we can summarize the available information as follows: (a) EIBAFE is a connectivity train which is either 8-9-10-11-12-13 or 13-12-11-10-9-8, (b) peak H is either CG7 or GC14, and (c) peak D is either GC14 or CG7. To resolve this symmetrical ambiguity and establish chain polarity, we next irradiated peak H and peak D separately as shown in Figure 5. In addition to cross-saturating E, peak D also gave a strong NOE to G (a GC pair). Peak H, besides cross-saturating E, also gave a weak NOE to peak C at 13.6 ppm (an AT pair—actually three AT pairs at 7 °C). Thus we tentatively concluded that H is GC14 (next to AT15) whereas D is probably CG7 (next to CG6). The fact that H resonates 0.4 ppm to higher field than D is also consistent with the expected larger nearest-neighbor ring-current shifts on GC14 than on CG7 (Arter & Schmidt, 1976), but again this rationalization is only valid if one assumes a right-handed B-DNA helix.

The tentative nature of the H to C NOE and the indirect nature of the ring-current shift assumptions prompted us to investigate more rigorous and direct methods of corroborating the  $\text{E}_1\text{-D-G}$  and  $\text{E}_2\text{-H-C}$  connectivities. To do this we irradiated peak I for longer time periods in order to take advantage of spin diffusion. The hope was that, by pumping the imino proton of I, we could “heat up” several protons of only the  $\text{E}_1$  component of peak E which in turn would partially cross-saturate the next nearest neighbors of I by a second-order spin-diffusion effect. The results are shown in Figure 6.

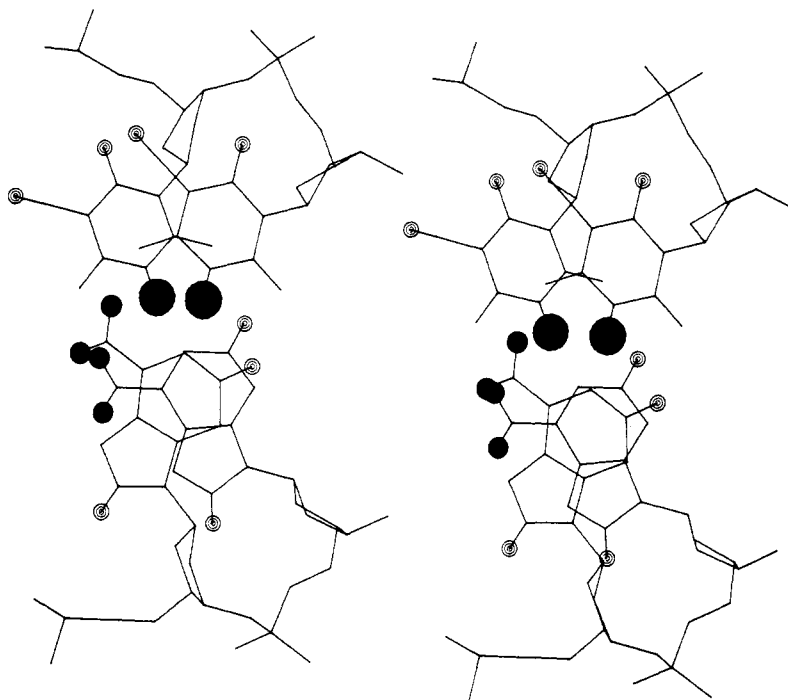


FIGURE 4: Stereoview of the stacking geometry of AT10 and AT11. The convention for proton types is as in Figure 2. The adenine C2H protons are shown to the right of the imino protons in the minor groove. AT10 is further from the viewer with its imino proton below and to the right of the closer AT11 imino proton. In three dimensions it is obvious that the AT10 imino proton is close to the C2H protons of both AT10 and AT11 whereas the AT11 imino proton is only close to its own C2H. The geometry of the two AT pairs is based on the crystal coordinates of dCGCGAATTCGCG (Dickerson & Drew, 1981).

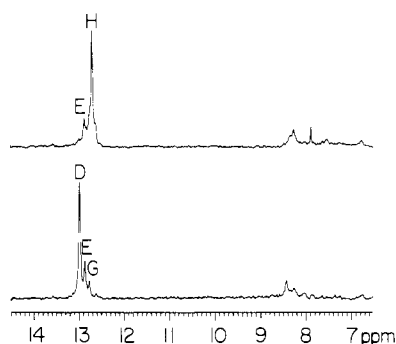


FIGURE 5: NOEs from peak H and peak D. From the small nearest-neighbor C2H NOE at 7.9 ppm, it is apparent that H is adjacent to an AT pair whereas D is not.

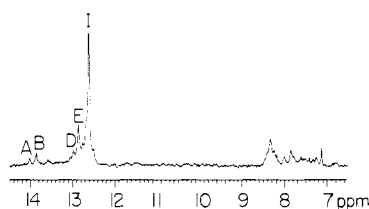


FIGURE 6: Spin-diffusion effects of long-term (1.2 s) saturation of peak I. Compared to Figure 3 the nearest-neighbor first-order effects on B and E are more pronounced, and next-to-nearest-neighbor second-order effects on A and D are now apparent.

When peak I was held saturated for 1.2 s, the extent of cross-saturation of the two neighbors B and E was increased (compare with top spectrum of Figure 3); however, second-order NOEs to A through B and to D via E were now detectable. Thus D and I are next nearest neighbors of each other with  $E_1$  between them, and hence F and H are the other pair of next nearest neighbors with  $E_2$  between them. The connectivity train is therefore D- $E_1$ -I-B-A-F- $E_2$ -H, with D and H both being GC pairs. The chain polarity can now be established from the NOEs produced by saturating D and H

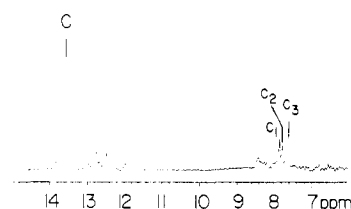


FIGURE 7: NOE from the multiple proton peak C. In the 7-9 ppm region three distinct narrow adenine C2H NOEs, labeled  $C_1$ ,  $C_2$ , and  $C_3$ , are observed, indicating the presence of three AT pairs in peak C.

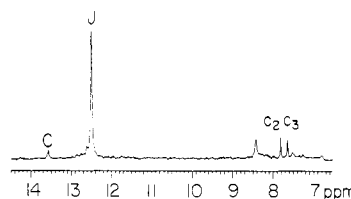


FIGURE 8: NOE from peak J. Both nearest neighbors of J appear to reside in peak C, and this is corroborated by the cross-saturation of both  $C_2$  and  $C_3$  in the 7-9 ppm region.

separately. Peak D produces large NOEs to G and E, neither of which contain an AT pair. This suggests that peak D is GC7 which has GC6 and GC8 as neighbors. Peak H on the other hand is adjacent to an AT pair since it cross-saturates a proximal C2H (7.9 ppm) and an AT imino proton in peak C (13.5 ppm). Thus D is between two GC pairs whereas H has a GC neighbor and an AT neighbor. This establishes that D is GC7 and H is GC14 (next to AT15). Hence the string G-D- $E_1$ -I-B-A-F- $E_2$ -H-C corresponds to base pairs CG6-CG7-GC8-CG9-AT10-AT11-GC12-GC13-GC14-AT15.

This now leaves peak J and the additional protons in peak C unassigned. To sort out the AT pairs whose imino protons overlap in peak C, we characterized them on the basis of the chemical shifts of their adenine C2H protons. As shown in Figure 7, saturation of peak C reveals the presence of at least

three AT pairs with C2H chemical shifts of 7.9, 7.8, and 7.6 ppm which we designate as originating from AT pairs C<sub>1</sub>, C<sub>2</sub>, and C<sub>3</sub>, respectively. The NOE from peak H to the 7.9 ppm CH resonance established that AT15 corresponds to C<sub>1</sub>. The effects of saturating peak J are shown in Figure 8. A large NOE to peak C is observed, suggesting that J may be cross-saturating more than one line in peak C. This suspicion is strongly corroborated by the appearance of two resolved adenine C2H NOEs at 7.8 ppm (C<sub>2</sub>) and at 7.6 ppm (C<sub>3</sub>). It is worth pointing out that the C2H's of these AT pairs (C<sub>2</sub> and C<sub>3</sub>) still show observable NOEs from adjacent neighbors even though their imino N3H is exchanging rapidly with solvent. Thus J is surrounded by AT pairs on either side and must therefore be CG4. Peak G (CG6) saturates the adenine CH at 7.6 ppm (C<sub>3</sub>), thus establishing the C<sub>3</sub> is AT5 and C<sub>2</sub> is TA3. Thus the entire connectivity train C<sub>2</sub>-J-C<sub>3</sub>-G-D-E-I-B-A-F-E-H-C<sub>1</sub> assigns base pairs 3-4-5-6-7-8-9-10-11-12-13-14-15 and accounts for the observed 13 protons in the imino spectrum. At 7 °C in the absence of added salt the imino protons of TA1, AT2, TA16, and AT17 are absent, presumably due to terminal fraying and rapid solvent exchange.

#### Discussion

As relative newcomers to the field of organic synthesis of DNA, we have found the solid-phase phosphite triester approach to be a very efficient and clean method for making preparative amounts of duplexes with defined sequences. Interresidue coupling is essentially complete in only 5 min whereas the phosphate triester approach requires coupling times of ca. 3 h (Dembek et al., 1981). Besides there is no danger of side reactions with G, T, or U residues with the strong coupling reagent MSNT [(1-mesitylene-2-sulfonyl)-3-nitro-1,2,4-triazole] which is used in the phosphate triester method (Jones et al., 1981). This side reaction can be quite appreciable, and in fact Sung (1981) has taken advantage of it to prepare 5-methylcytidine from thymidine. No strong coupling reagents are required in the phosphite approach; a well-separated, clean major product is routinely observed on final workup by TLC. A possible cause for caution is the reported glycosidic cleavage (especially of deoxyadenosine) by the trichloroacetic acid used to remove the dimethoxytrityl group from the 5' end of the chain in each cycle of the synthesis (T. P. Patel et al., 1982). However, depurination has not been a significant problem in our hands in that we have now made different oligonucleotides ranging in size from 10 to 20 base pairs, and in each case the integrated value of each AT imino proton NMR signal is the same as the unit GC imino proton intensity.

The usefulness of custom synthesis with complete control over the identity of any residue in studying the correlation of structure and dynamics with function in regulatory DNA sequences is obvious. With such a complete synthesis and imino proton assignment for an *entire* biological operator DNA sequence, it is now possible to proceed to a study of the precise thermal unfolding sequence as well as the helix-coil dynamics at each position in the operator sequence by using currently available time-resolved double-resonance NMR techniques (Johnston & Redfield, 1981; Hurd & Reid, 1980). Such investigations are currently in progress in this laboratory.

When combined with parallel studies on genetically identified nonfunctional point mutations, the results should shed a great deal of light on the physical basis of operator function and recognition by repressor.

In the final stages of this paper, we learned of similar work on O<sub>R</sub>3 by the Markley and Gilham research groups at Purdue University (E. Ulrich et al., personal communication).

**Registry No.** dTATCACCGCAAGGGATA, 84991-72-0; dTATCCCTTGCGGTGATA, 84842-47-7; dTATCACCGCAAGGGATA-dTATCCCTTGCGGTGATA, 85762-02-3.

#### References

- Arter, D. B., & Schmidt, P. G. (1976) *Nucleic Acids Res.* 3, 1437.  
Beaucage, S. L., & Caruthers, M. H. (1981) *Tetrahedron Lett.* 22, 1859.  
Bourgeois, S., & Pfahl, M. (1976) *Adv. Protein Chem.* 30, 1.  
Chow, F., Kempe, T., & Palm, G. (1981) *Nucleic Acids Res.* 9, 2807.  
Dembek, P., Miyoshi, K., & Itakura, K. (1981) *J. Am. Chem. Soc.* 103, 706.  
Dickerson, R. E., & Drew, H. R. (1981) *J. Mol. Biol.* 149, 761.  
Feigon, J., Wright, J. M., Leupin, W., Denny, W. A., & Kearns, D. R. (1982) *J. Am. Chem. Soc.* 104, 5541.  
Hare, D. R., & Reid, B. R. (1982a) *Biochemistry* 21, 1835.  
Hare, D. R., & Reid, B. R. (1982b) *Biochemistry* 21, 5129.  
Hurd, R. E., & Reid, B. R. (1980) *J. Mol. Biol.* 142, 181.  
Johnston, P. D., & Redfield, A. G. (1981) *Biochemistry* 20, 3996.  
Jones, S. S., Reese, C. B., Sibanda, S., & Ubasawa, A. (1981) *Tetrahedron Lett.* 22, 4755.  
Matteucci, M. D., & Caruthers, M. H. (1981) *J. Am. Chem. Soc.* 103, 3186.  
Narang, S. A., Brousseau, R., Hsiung, H. M., & Michniewicz, J. J. (1980) *Methods Enzymol.* 65, 61.  
Ohlendorf, D. H., Anderson, W. F., Fisher, R. G., Takeda, Y., & Matthews, B. W. (1982) *Nature (London)* 298, 718.  
Patel, D. J., Kozlowski, S. A., Marky, L. A., Broka, C., Rice, J. A., Itakura, K., & Breslauer, K. J. (1982) *Biochemistry* 21, 428.  
Patel, T. P., Millican, T. A., Bose, C. C., Titmas, R. C., Mock, G. A., & Eaton, M. A. W. (1982) *Nucleic Acids Res.* 10, 5605.  
Ptashne, M., Jeffrey, A., Johnson, A. D., Maurer, R., Meyer, B. J., Pabo, C. O., Roberts, T. M., & Sauer, R. T. (1980) *Cell (Cambridge, Mass.)* 19, 1.  
Reid, B. R. (1981) *Annu. Rev. Biochem.* 50, 969.  
Roy, S., Papastavros, M. Z., & Redfield, A. G. (1982) *Biochemistry* 21, 6081.  
Sung, W. L. (1981) *Nucleic Acids Res.* 9, 6139.  
Tanaka, T., & Letsinger, R. L. (1982) *Nucleic Acids Res.* 10, 3249.  
Ti, G. S., Gaffney, B. L., & Jones, R. A. (1982) *J. Am. Chem. Soc.* 104, 1316.  
Zuiderweg, E. R. P., Scheek, R. M., Veeneman, G., van Boom, J. H., Kaptein, R., Ruterjans, R., & Beyreuther, K. (1981) *Nucleic Acids Res.* 9, 6553.